Proceedings of the ASME 2010 3rd Joint US-European Fluids Engineering Summer Meeting and
8th International Conference on Nanochannels, Microchannels, and Minichannels
FEDSM-ICNMM2010
August 1-5, 2010, Montreal, Canada

FEDSM-ICNMM2010-30036

THE FLOW AROUND AN IMPULSIVELY STARTED SQUARE PRISM

Nelson Tonui
Department of Mechanical Engineering
University of Saskatchewan
57 Campus Drive, Saskatoon,
Saskatchewan, Canada, S7N 5A9

David Sumner
Department of Mechanical Engineering
University of Saskatchewan
57 Campus Drive, Saskatoon,
Saskatchewan, Canada, S7N 5A9

ABSTRACT

The flow around a square prism impulsively set into motion was studied experimentally using particle image velocimetry (PIV). The experiments were conducted in an X-Y towing tank for Reynolds numbers from Re = 200 to 1000 and dimensionless acceleration parameters from a^* = 0.5 to 10. The temporal development of the near-wake recirculation zone, and its pair of primary eddies, was examined from the initial start until the wake became asymmetric. When considering the time elapsed from the start of motion, the temporal development of the wake was sensitive the initial acceleration. "Impulsively started" conditions were effectively attained for $a^* \geq 3$. However, when considering the distance traveled from the start of motion, the wake parameters were sensibly independent of a^* for $a^* \geq 0.5$. Concerning the temporal development of the recirculation zone, the length of the recirculation zone, the streamwise location of the primary eddies, and the strength of the primary eddies increased with time following the impulsive start, while the cross-stream spacing of the eddy centres remained nearly constant. The recirculation zone of the square prism was longer than that of the impulsively started circular cylinder but shorter than an impulsively started flat plate. For $t^* > 2$, the primary eddy strength, maximum vorticity, and cross-stream spacing of the primary eddies were the same for both the square prism and circular cylinder.

1. INTRODUCTION

The flow around an impulsively started circular cylinder is one of the classic examples of unsteady fluid dynamics. The flow is often used as a benchmark for the testing and validation of numerical simulations. A wide range of experimental studies [1-12] and numerical simulations [13-21] can be found in the literature, for Reynolds numbers up to and greater than Re = UD/ν = 10,000 (where D is the diameter of the cylinder, U is the steady cylinder velocity attained following the impulsive start, and ν is the kinematic viscosity of the fluid). Together, these studies provide a detailed description of the temporal development of the cylinder wake, through flow visualization and numerical simulations, and the behaviour of the unsteady lift and drag forces.

The flow field of the impulsively started circular cylinder is characterized by the formation of a symmetrical recirculation zone in the near wake. The recirculation zone contains a pair of stationary primary eddies of equal strength and opposite rotation. As the dimensionless elapsed time from the start of motion, $t^* = tU/D$ (where t is the elapsed time), approaches t^* = 4 or 5, the recirculation zone becomes asymmetric and the primary eddies are eventually shed from the cylinder. Provided the Re is sufficiently high, the familiar steady flow pattern of periodic Kármán vortex shedding is then initiated. The flow field may also be marked by small regions of secondary vorticity located downstream of the separation points.

The flow field of an impulsively started square prism (of side length, D) is similar to that of the circular cylinder. A schematic of the flow field is shown in Fig. 1, where the length of the recirculation zone, L_R, is measured from the rear of the prism (in the streamwise direction, x). The centres of the primary eddies are denoted by the streamwise position from the rear of the prism, a, and the transverse spacing, b (in the cross-stream direction, y).

Compared to the case of the impulsively started circular cylinder, there have been relatively few studies of the flow around an impulsively started square prism and other sharp-edged bluff bodies. Davis and Moore [22] performed numerical simulations of the flow around rectangular prisms at different angles of attack for Re = 100 to 2800. Although they considered the behaviour of the aerodynamic forces following

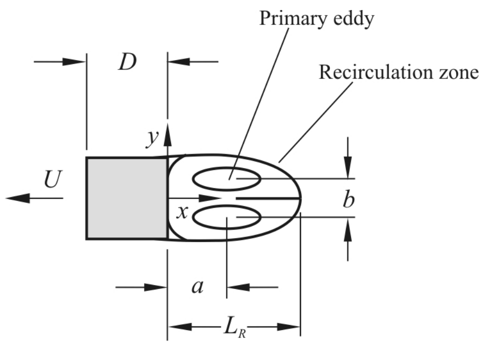

Figure 1. Schematic of flow around an impulsively started square prism at Re = 500 and *t = 3.**

an impulsive start, most of the analysis was focused on steady flow conditions at much higher elapsed times, when Kármán vortex shedding had been initiated. Sarpkaya and Ihrig [23] performed experiments (at Re = 20,000) and numerical simulations on the impulsively started flow around rectangular prisms at different incidence angles. The primary focus of their study was the behaviour of the force coefficients with time, from the moment of impulsive start up to and beyond the occurrence of Kármán vortex shedding. Finaish [10] performed a flow visualization study of an impulsively started square cylinder at Re = 200 and recorded the flow development from the early stages of the flow up to the vortex shedding regime. The results were qualitative in nature and no measurements were made of the recirculation zone and its primary eddies. Lee et al. [24] performed numerical simulations of impulsively started flow around a square prism for Re = 25 to 1000. In this study, the numerical simulations were not validated against any experimental data, mainly because of an absence of such data in the literature. Impulsively started flow around a flat plate, as another example of a sharp-edged bluff body, has been studied experimentally by Polidori et al. [25] and numerically by Koumoutsakos and Shiels [26]. These studies were focused on the development of the near wake recirculation zone.

The present study addresses the lack of experimental data for the impulsively started square prism, and provides a new dataset for validating numerical simulations of flows around sharp-edged bluff bodies. An experimental investigation is conducted of the flow around impulsively started square prisms for Re = 200 to 1000 using particle image velocimetry (PIV). The study is focused on the temporal development of the near-wake recirculation zone, and the primary eddies, up until the flow field becomes asymmetric.

NOMENCLATURE

a	acceleration [mm/s^2], streamwise location of the primary eddies from the rear of the prism [mm]
a^*	dimensionless acceleration parameter
AR	aspect ratio
b	transverse spacing of the centres of the primary eddies [mm]
D	prism side length [mm]
L	length of prism [mm]
L_R	length of the recirculation zone measured from the rear of the prism [mm]
Re	Reynolds number
S	distance traveled from the start of motion [mm]
t	time [s]
t^*	dimensionless time
U	steady freestream or towing (prism) velocity [mm/s]
u	streamwise velocity component [mm/s]
v	transverse velocity component [mm/s]
x	streamwise coordinate
y	transverse coordinate [mm]
Γ	circulation or vortex strength [m^2/s]
Γ^*	dimensionless circulation or vortex strength
ν	kinematic viscosity [m^2/s]
ω	vorticity [s^{-1}]
ω^*	dimensionless vorticity
ω_{max}	maximum vorticity [s^{-1}]
ω^*_{max}	dimensionless maximum vorticity

2. EXPERIMENTAL APPROACH

The experiments were conducted in water in an X-Y towing tank (Fig. 2) with internal dimensions of 3.96 m long, 1.03 m wide, and 0.75 m deep. The glass side walls, end walls, and floor of the towing tank give optical access for PIV measurements. The primary towing direction (X-direction, 3.5 m of travel) is along the length of the tank, where the main carriage straddles the tank width and moves on two parallel rails. A linear motion stage containing the secondary carriage is mounted on the main carriage for transverse movement across the tank (Y-direction, 260 mm of travel). The secondary carriage is mounted between two rails and is driven by a lead screw and stepping motor.

The motion control system for the X-Y towing tank includes a personal computer, a National Instruments (NI) PCI-7344 motion controller card, two Intelligent Motion Systems IM1007 micro-step drivers, and a NI UMI-7764 universal motion interface. Encoders on both axes provide closed-loop position feedback, while home and limit switches used on both axes control the start and end positions for the motion trajectories. The user interface was developed in the LabVIEW programming language.

In the present experiments, only the secondary carriage (Y-direction) was used. A square prism with D = 25.4 mm was immersed in the water vertically from beneath the Y-motion stage (Fig. 2). The working depth of water was 720 mm. There was a gap of 16 mm (0.63D) between the end of the prism and the bottom of the tank, giving an aspect ratio of AR = $L/D \approx 28$ (where L is the length of the prism immersed in the water).

Velocity field measurements were made with a TSI PIV system. The laser light (532 nm) was supplied by a 120-mJ/pulse dual Nd:YAG Gemini PIV 15 laser from New Wave Research, which had a maximum pulse frequency of 15 Hz.

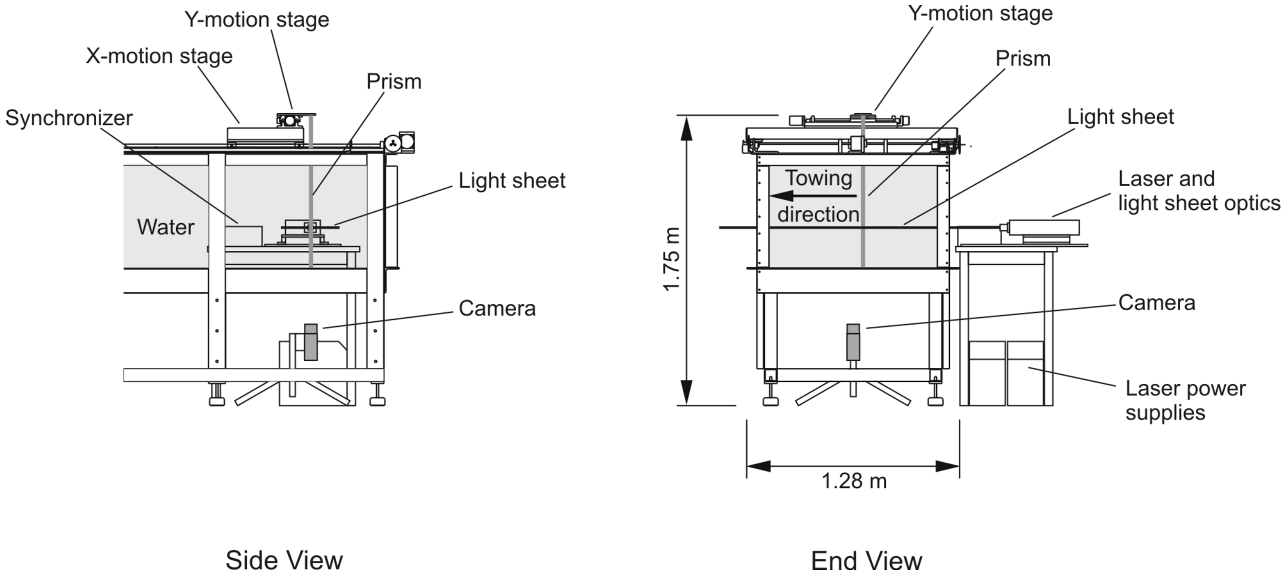

Figure 2. The experimental set-up for the PIV experiments in the X-Y towing tank (only a partial side view of the tank is shown). The square prism is suspended vertically in the water from beneath the Y-motion stage. The laser light sheet forms a horizontal plane that intersects the prism normal to its axis. The prism is towed from right to left, as shown in the end view. The camera remains in a fixed position beneath the tank.

The light sheet optics included a −50-mm cylindrical lens and a 1000-mm spherical lens. The light sheet was aligned horizontally normal to the prism axis (Fig. 2) and was located 294 mm (11.6*D*) above the lower end of the prism.

A TSI PowerView Plus 2MP (2 Megapixel) cross-correlation camera with a 50-mm Nikon lens was mounted vertically in a fixed position beneath the towing tank. Images were captured by a 64-bit frame grabber on a computer workstation. The timing of the lasers, camera, and frame grabber was controlled by a TSI LaserPulse synchronizer, TSI Insight 3G software, and a reference signal supplied by the motion control system at the start of the prism motion. The water was seeded with 8-12-μm hollow glass spheres. Image pairs were processed with the Insight 3G software's single-pass Nyquist grid algorithm, Hart correlation algorithm, and bilinear peak detection algorithm. The interrogation window was 56×56 pixels and 50% overlap was used. The field of view was approximately 92×68 mm. The resulting velocity vector field was typically 56×41 vectors, with a vector spacing of approximately 0.065*D*.

The experiments were conducted at Re = 200, 300, 500, and 1000, which corresponded to towing speeds of $U \approx 8$, 12, 20, and 40 mm/s, respectively. In addition, the acceleration parameter was varied from $a^* = 0.5$ to 10, which corresponded to constant acceleration values of $a \approx 8$ to 157 mm/s^2. For each Re and a^* combination, the PIV system was used to obtain the time history of the instantaneous in-plane velocity field (u and v components, in the x and y coordinate directions, respectively) and in-plane vorticity field (ω_z, expressed in dimensionless form as $\omega_z^* = \omega_z D/U$) as the flow developed over from $t^* = 0$ to 5.

3. FLOW FIELD

The temporal development of the in-plane velocity and vorticity fields for the impulsively started square prism is shown in Fig. 3, for the specific case of Re = 500 and $a^* = 5$. Each field represents an instantaneous velocity or vorticity field; no ensemble averaging was performed. For all values of Re and a^*, the flow field remained symmetric until $t^* = 4$ to 5. In contrast, the numerical simulations of Lee et al. [24] did not show any asymmetry up to the end of the simulation time, at $t^* = 8$.

As the prism moves through the fluid following the impulsive start, the separated flow follows the upper and lower surfaces of the prism and merges into the growing vorticity concentrations that denote the recirculation zone and its primary eddies. The recirculation zone elongates in the streamwise direction with increasing t^* and small concentrations of secondary vorticity form on the back face of the prism close to the rear corners (Fig. 3).

4. INFLUENCE OF INITIAL ACCELERATION

A comparison of the wake for two values of acceleration parameter, $a^* = 1$ and $a^* = 5$, is shown in Fig. 4. It can be seen that the length of the recirculation zone develops slower for the lower acceleration parameter. From the velocity fields, several wake parameters were determined and are shown (for the case of Re = 500) plotted against elapsed time, t^*, and distance traveled, S/D, in Figs. 5 and 6, respectively.

4.1. Time Elapsed from the Start of Motion

The length of the recirculation zone (Fig. 5a) increases with elapsed time following the impulsive start. At a given t^*,

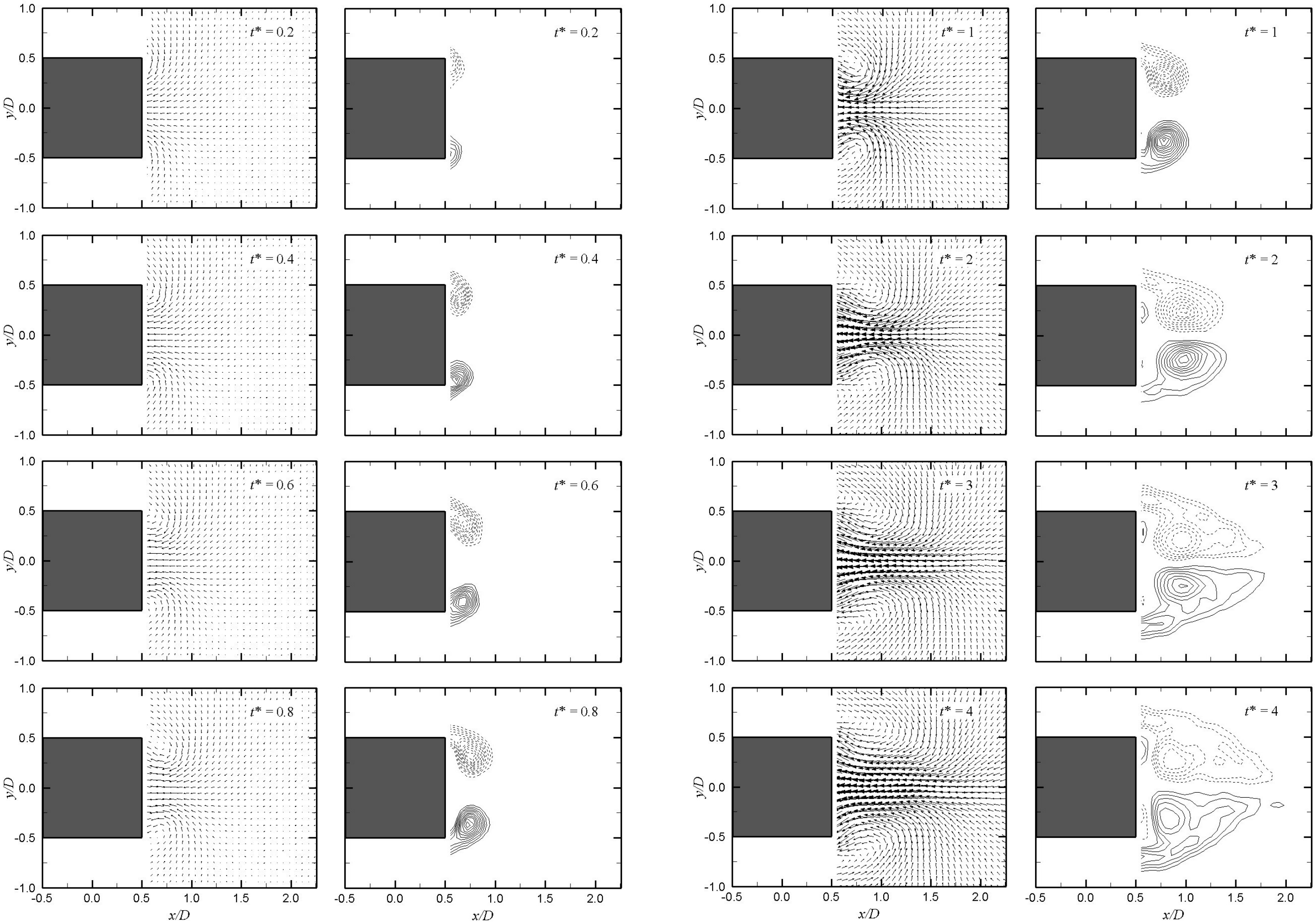

Figure 3. Temporal development of the flow field for an impulsively started square prism, Re = 500, a^* = 5. Contour lines of constant ω^*; minimum contour $|\omega^*|$ = 2; contour increment $\Delta\omega^*$ = 1; dashed lines represent negative (clockwise) vorticity.

the recirculation zone length increases with a^* until $a^* \geq 3$, at which point the data become independent of further increases in a^*. This suggests that the flow can be considered impulsively started once $a^* \geq 3$, which is consistent with results for a circular cylinder [27].

The circulation (strength) of a primary eddy, Γ^* (Fig. 5b), increases with both t^* and a^*. For a given value of t^*, the eddy strength increases with a^*. The circulation values for $a^* \geq 3$ are seen to merge to a single curve, indicating impulsively started conditions have been attained.

The streamwise location of the centres of the primary eddies (Fig. 5c) behaves similarly to the length of the recirculation zone (Fig. 5a). As the primary eddies grow with the elapsed of time following the impulsive start, the centres of the eddies move farther away from the rear of the prism. At a given t^*, the eddy centres are located closer to the prism at lower values of a^*. Similar to the L_R/D data (Fig. 5a), the a/D data collapse onto a common curve when $a^* \geq 3$, indicating that impulsively started conditions have been attained. The transverse (cross-stream) spacing of the eddies (Fig. 5d) is generally independent of a^*.

The maximum vorticity (Fig. 5e) within the recirculation zone attains a peak value shortly after the start of motion, and then slowly decreases with the elapsed time. The ω^*_{max} profiles for the higher a^* values can be seen to nearly collapse onto one curve, an indication that conditions similar to impulsively started motion have been reached.

4.2. Distance Traveled from the Start of Motion

For a constant value of acceleration (which is essentially the case in the present experiments), the acceleration period will be completed after an elapsed time of $t^* = 1/a^*$, after which the prism will have traveled a distance of $S/D = 1/(2a^*)$. Thus, for a^* = 10 (the highest acceleration parameter considered in these experiments), the prism will have traveled a relative distance of S/D = 0.05 after an elapsed time of t^* = 0.1. For a^* = 0.5 (the smallest acceleration parameter considered in

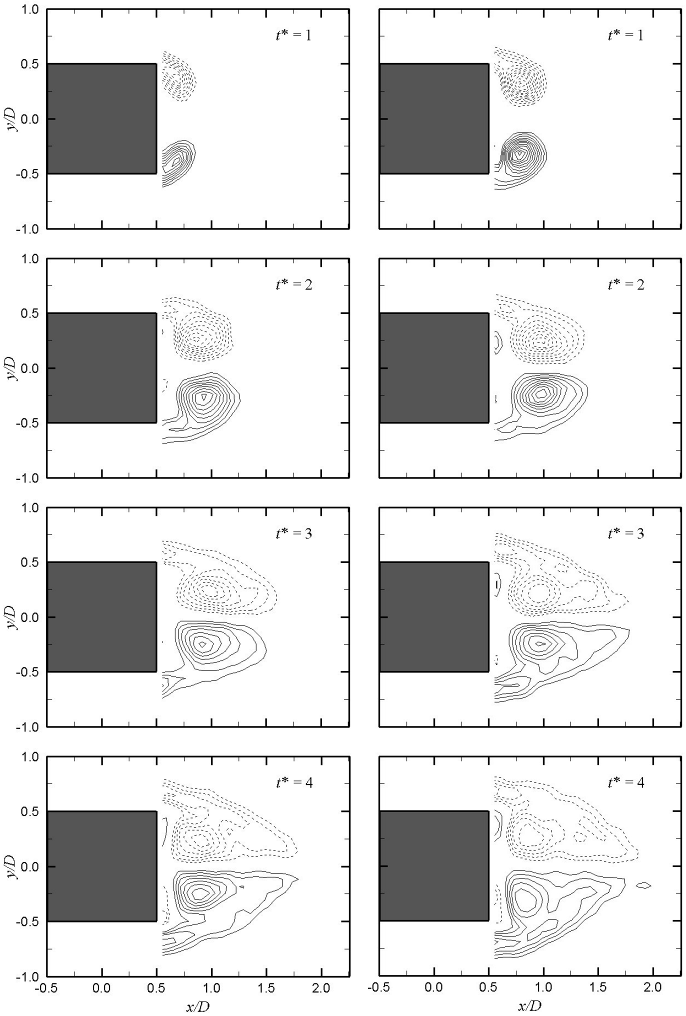

Figure 4. Temporal development of flow field for an "impulsively started" square prism, Re = 500: (a) a^* = 1; (b) a^* = 5. Contour lines as in Figure 3.

these experiments), the prism will have traveled a relative distance of $S/D = 1$ after an elapsed time of $t^* = 2$.

In Fig. 6, the wake parameters are plotted against distance traveled by the square prism, S/D, rather than against the time elapsed from the start of motion, t^* (as shown in Fig. 5). The data for different acceleration parameters collapse onto common curves. This shows that the wake of a non-impulsively started square prism depends primarily on the distance traveled by the prism from its starting position, rather than on the initial acceleration phase (or the prism's velocity time-history). The collapse of the data with S/D indicates that impulsively started flow conditions are attained for all values of acceleration parameter considered in these experiments, i.e., for $a^* \geq 0.5$, consistent with similar studies of the circular cylinder [11, 27].

5. INFLUENCE OF REYNOLDS NUMBER

Recirculation zone data for impulsively started conditions ($a^* = 5$) and for Re = 200 to 1000 are shown in Fig. 7. Data are also shown for an impulsively started circular cylinder obtained in the same test facility. Some published data from [25, 26] are also shown for other sharp-edged bodies. For the square prism, the behaviour of the recirculation zone parameters (Fig. 7) was mostly independent of Re over the range tested, Re = 200 to 1000. However, for Re = 200, the length of the recirculation zone (Fig. 7a) and the streamwise location of the primary eddies (Fig. 7c) continue to grow rapidly with elapsed time, whereas for Re = 500 and 1000 the growth slows and begins to reduce for $t^* > 3$. An intermediate trend is seen at Re = 300.

6. COMPARISON WITH OTHER IMPULSIVELY STARTED BLUFF BODIES

From Fig. 7a, it is seen that the recirculation zone for the square prism, at a given value of t^*, is longer than that for the circular cylinder but shorter than those of the flat plate and semi-circular prism (with a rounded forebody). The longest recirculation zone is for the flat plate, which has fixed separation points (at the upper and lower ends of the plate) and an absence of both a forebody and afterbody (which strongly influence a bluff body's wake development and characteristics). A rounded forebody (the semi-circular prism) reduces the length of the recirculation zone, since the geometry allows the separation points to move over the forward surfaces of the body. The square prism, because of its thickness, might be considered as a flat plate with an afterbody and corresponds to a shorter recirculation zone. The geometry with both a rounded forebody and afterbody (the circular cylinder) likewise has the shortest recirculation zone.

It is also noted from Fig. 7a that the growth of the recirculation zone length for the square prism eventually slows, such that its length coincides with that of the circular cylinder as the flow approaches asymmetry.

For both the square prism and the circular cylinder, the circulation of the primary eddies (Fig. 7b) increases almost linearly with time. For $t^* < 2$, the primary eddies of the square prism are stronger than those of the circular cylinder.

The streamwise location of the centres of the primary eddies (Fig. 7c) behaves similarly to length of the recirculation zone (Fig. 7a). The cross-stream spacing of the primary eddy centres (Fig. 7d) is approximately the body width at initial t^* values but approaches the value for the circular cylinder when $t^* > 2$.

Fig. 7e shows a comparison of the maximum vorticity data. The curves for the different Re and for the square prism and circular cylinder have the same characteristics. Considering the data for Re = 1000, the peak value is attained more rapidly for the square prism, at $t^* \approx 1$, compared to the circular cylinder, at $t^* \approx 2.25$. For $t^* > 2$, the maximum vorticity for the square prism becomes the same as that of the circular cylinder, similar to what was observed for the circulation (Fig. 7c).

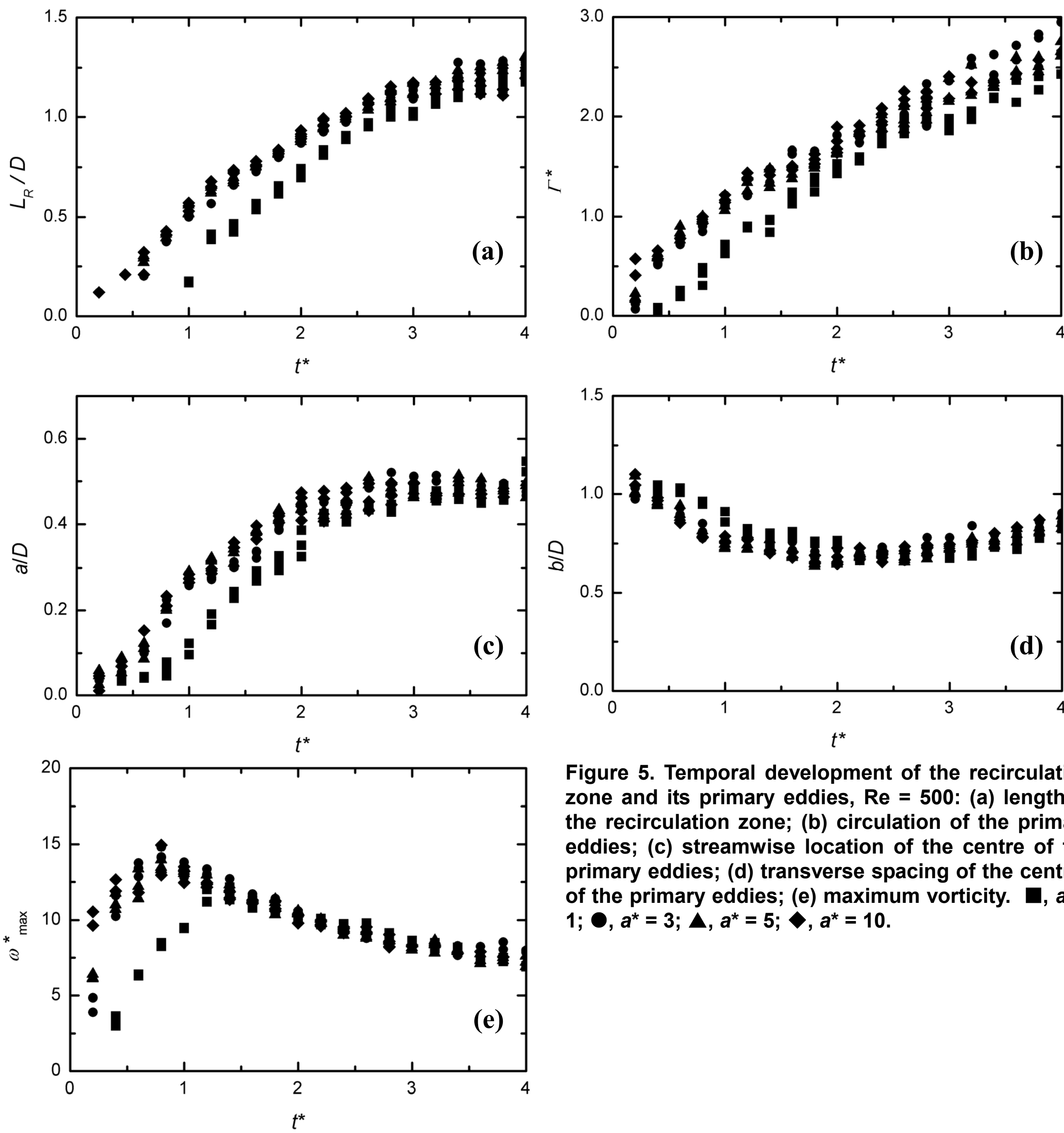

Figure 5. Temporal development of the recirculation zone and its primary eddies, Re = 500: (a) length of the recirculation zone; (b) circulation of the primary eddies; (c) streamwise location of the centre of the primary eddies; (d) transverse spacing of the centres of the primary eddies; (e) maximum vorticity. ■, *a = 1; ●, *a** = 3; ▲, *a** = 5; ◆, *a** = 10.**

7. CONCLUSIONS

An experimental study of an impulsively started square prism at Re = 200 to 1000 was conducted using PIV for a^* = 0.5 to 10. The focus of the study was the temporal development of the recirculation zone and its primary eddies while the flow field remained symmetric. The data presented here are some of the first reported experimental results for the near-wake of an impulsively started square prism and may be useful for validating numerical simulations of flows around sharp-edged bluff bodies (particularly in cases where using the impulsively started circular cylinder as a benchmark flow might be computationally inconvenient, due to movement of the separation points or the type of grid employed). Some additional insight is also provided into the influence of body geometry (sharp edges, flat surfaces, forebody and afterbody shape) on the behaviour of bluff body wakes.

The experiments demonstrated that the temporal development of the wake is sensitive to the initial acceleration. At a given elapsed time from the start of motion, t^*, the length of the recirculation zone, the locations and strengths of the primary eddies within the recirculation zone, and the maximum values of vorticity within the primary eddies, were dependent on a^*. On the basis of the elapsed time from the start of motion, "impulsively started" conditions were effectively attained for $a^* \geq 3$, since at this point the wake parameters had become

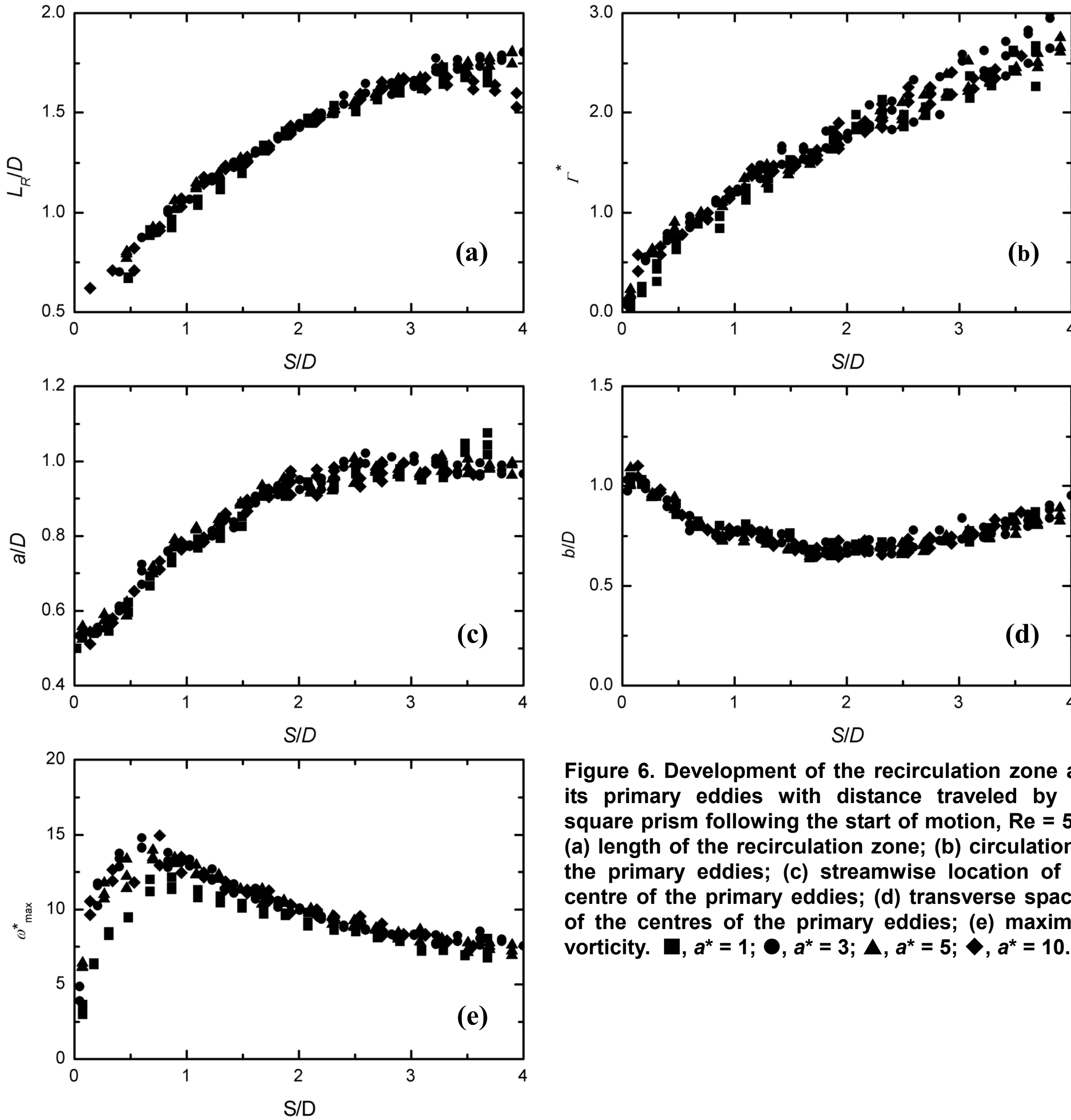

Figure 6. Development of the recirculation zone and its primary eddies with distance traveled by the square prism following the start of motion, Re = 500: (a) length of the recirculation zone; (b) circulation of the primary eddies; (c) streamwise location of the centre of the primary eddies; (d) transverse spacing of the centres of the primary eddies; (e) maximum vorticity. ■, a^* = 1; ●, a^* = 3; ▲, a^* = 5; ◆, a^* = 10.

insensitive to a^*. However, when considering the relative distance traveled by the prism from the start of motion, S/D, the wake parameters were found to be sensibly independent of a^* for $a^* \geq 0.5$; this result was consistent with [11, 27] for a circular cylinder. The experiments therefore showed that the development of the prism wake was more strongly a function of the distance traveled by the prism from the start of motion, S/D, rather than the acceleration.

The temporal development of the recirculation zone of the square prism is similar, in many respects, to the more familiar case of the circular cylinder. The length of the recirculation zone, the streamwise location of the primary eddies, and the strength of the primary eddies increased with time following the impulsive start, while the cross-stream spacing of the eddy centres remained nearly constant. Some Reynolds number sensitivity was observed for Re < 500. At a given value of t^*, the square prism typically had a longer recirculation zone, stronger primary eddies, and primary eddies located farther away from the prism, compared to the case of the circular cylinder. In terms of the recirculation zone length, the square prism results fall in between data for the impulsively started flat plate and the circular cylinder (alluding to the influence of forebody and afterbody geometry). For $t^* > 2$, the primary eddy strength, maximum vorticity, and cross-stream spacing of the primary eddies, were the same for both the square prism and circular cylinder. Small regions of secondary vorticity were observed to form on the rear surface of the prism.

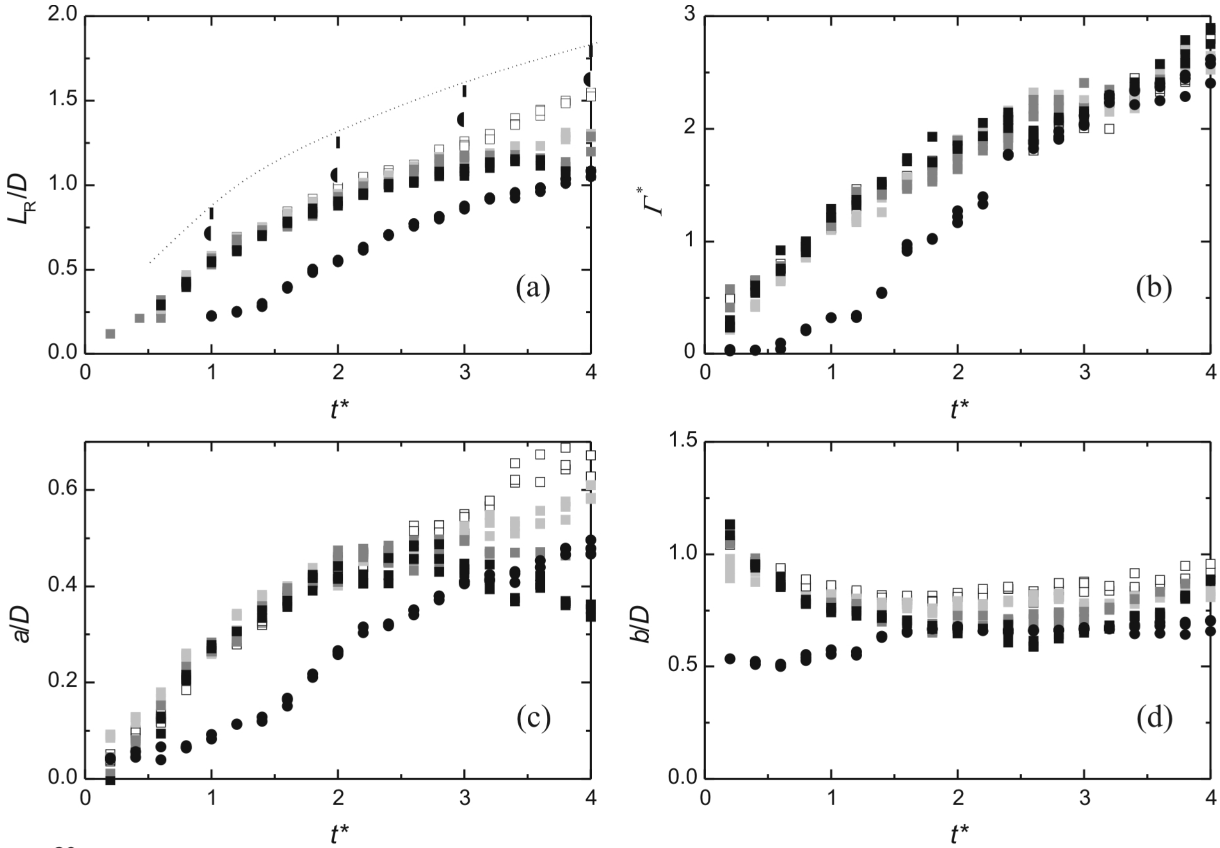

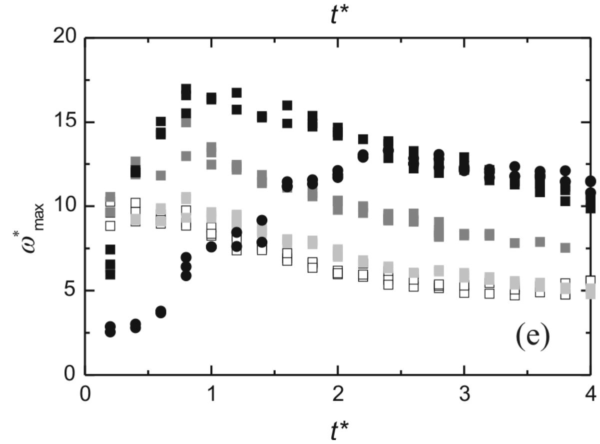

Figure 7. Development of the recirculation zone for an impulsively started square prism: (a) length of the recirculation zone; (b) circulation of the primary eddies; (c) streamwise location of the centre of the primary eddies; (d) transverse spacing of the centres of the primary eddies; (e) maximum vorticity. Square prism: □, Re = 200, *a = 5; ■, Re = 300, *a** = 5; ■, Re = 500, *a** = 5; ■, Re = 1000, *a** = 5. Circular cylinder: ●, Re = 1000, *a** = 5. Flat plate: ------, Re = 600 [26]; I, Re = 1000 [25]. Semi-circular prism (rounded forebody): ◖, Re = 1000 [25].**

ACKNOWLEDGMENTS

The authors acknowledge the support of the Natural Sciences and Engineering Research Council (NSERC) of Canada, the Canada Foundation for Innovation (CFI), and the Innovation and Science Fund of Saskatchewan. The assistance of D.M. Deutscher and Engineering Shops is appreciated.

REFERENCES

[1] Honji, H., and Taneda, S., 1969, "Unsteady Flow past a Circular Cylinder," Journal of the Physical Society of Japan, 27(6), pp. 1668-1677.

[2] Nagata, H., Kakehi, Y., Tsunekama, M., and Hasegawa, T., 1975, "Unsteady Flow Past a Circular Cylinder Started Impulsively," Bulletin of the JSME, 18, pp. 992-1001.

[3] Nagata, H., Minami, K., and Murata, Y., 1979, "Initial Flow Past an Impulsively Started Circular Cylinder," Bulletin of the JSME, 22, pp. 512-520.

[4] Nagata, H., Funada, H., Kawai, K, and Matsui, T., 1985a, "Unsteady Flows in the Vortex Region behind a Circular Cylinder Started Impulsively: 1st Report, Feeding Mechanism of Vorticity and Onset of Turbulence," Bulletin of the JSME, 28, pp. 2599-2607.

[5] Nagata, H., Funada, H., and Matsui, T., 1985b, "Unsteady Flows in the Vortex Region behind a Circular Cylinder Started Impulsively: 2nd Report, Velocity Fields and Circulations," Bulletin of the JSME, 28 (245), pp. 2608-2616.

[6] Nagata, H., Nagase, I., and Ito, K., 1989, "Unsteady Flows past a Circular Cylinder Started Impulsively in the

Reynolds Number Range $500 < Re < 10^4$ (The Structure of the Vortex Region and Feeding Mechanism of Vorticity)," JSME International Journal Series II, 32, pp. 540-549.
[7] Nagata, H. Ito, K., and Taniguchi, T., 1990, "Unsteady Flows past a Circular Cylinder Started Impulsively in the Reynolds Number Range $500 < Re < 10^4$ (The Pressure Distribution on the Surface of the Cylinder)," JSME International Journal Series II, 33, pp. 501-510.
[8] Coutanceau, M., and Bouard, R., 1977, "Experimental Determination of the Main Features of the Viscous Flow in the Wake of a Circular Cylinder in Uniform Translation. Part 2. Unsteady Flow," Journal of Fluid Mechanics, 79, pp. 257-272.
[9] Bouard, R., and Coutanceau, M., 1980, "The Early Stage of Development of the Wake behind an Impulsively Started Cylinder for $40 < Re < 10^4$," Journal of Fluid Mechanics, 101, pp. 583-607.
[10] Finaish, F., 1991, "On Vortex Structures and Processes over Bluff Bodies in Impulsive Flow," Experiments in Fluids, 11, pp. 262-267.
[11] Sarpkaya, T., 1991. "Nonimpulsively Started Steady Flow about a Circular Cylinder," AIAA Journal, 29(8), pp. 1283-1289.
[12] Chu, C.C., and Liao, Y.Y., 1992, "A Quantitative Study of the Flow around an Impulsively Started Circular Cylinder," Experiments in Fluids, 13, pp. 137-146.
[13] Loc, T.P., and Bouard, R., 1985, "Numerical Solution of the Early Stage of the Unsteady Viscous Flow around a Circular Cylinder: A Comparison with Experimental Visualization and Measurements," Journal of Fluid Mechanics, 160, pp. 93-177.
[14] Smith, P.A., and Stansby, P.K., 1988, "Impulsively Started Flow around a Circular Cylinder by the Vortex Method," Journal of Fluid Mechanics, 194, pp. 45-77.
[15] Chang, C.C., and Chern, R.L., 1991, "A Numerical Study of Flow around an Impulsively Started Circular Cylinder by a Deterministic Vortex Method," Journal of Fluid Mechanics 233, pp. 243-263.
[16] Koumoutsakos, P., and Leonard, A., 1995, "High-Resolution Simulations of the Flow around an Impulsively Started Cylinder Using Vortex Methods," Journal of Fluid Mechanics, 296, pp. 1-38.
[17] Nair, M.T., and Sengupta, T.K., 1996, "Onset of Asymmetry: Flow past Circular and Elliptic Cylinders," International Journal for Numerical Methods in Fluids, 23, pp. 1327-1345.
[18] Cheng, M, Chew, Y.T., and Luo, S.C., 1997, "A Hybrid Vortex Method for Flows over a Bluff Body," International Journal for Numerical Methods in Fluids, 24, pp. 253-274.
[19] Li, Y., Shock, R., Zhang, R., and Chen, H., 2004, "Numerical Study of Flow past an Impulsively Started Cylinder by Lattice-Boltzmann Method," Journal of Fluid Mechanics, 519, pp. 273-300.
[20] Sanyasiraju, Y.V.S.S., and Manjula, V., 2005, "Flow Past an Impulsively Started Circular Cylinder Using a Higher-Order Semicompact Scheme," Physical Review E, 72, 016709.
[21] Dupuis, A., Chatelain, P., and Koumoutsakos, P., 2008, "An Immersed Boundary-Lattice-Boltzmann Method for the Simulation of the Flow past an Impulsively Started Cylinder," Journal of Computational Physics, 227, pp. 4486-4498.
[22] Davis, R.W., and Moore, E.F., 1982, "A Numerical Study of Vortex Shedding from Rectangles," Journal of Fluid Mechanics, 116, pp. 475-506.
[23] Sarpkaya, T., and Ihrig, C.J., 1986, "Impulsively Started Steady Flow about Rectangular Prisms: Experiments and Discrete Vortex Analysis," ASME Journal of Fluids Engineering, 108, pp. 47-54.
[24] Lee, T.S., Tan, R.S., and Xu, X.P., 1996, "Numerical Study of the Early Stages of Impulsively Started Unsteady Laminar Flow Past a Square Cylinder," International Journal of Numerical Methods for Heat and Fluid Flow, 6, pp. 53-70.
[25] Polidori, G., Pineau, G., Abed Meraim, K., Coutanceau, M., 1992, "Shedding Process of the Initial Vortices from Impulsively Started Cylinders at Re = 1000: End and Body Geometry Effects," Proceedings, Bluff-Body Wakes, Dynamics and Instabilties, IUTAM Symposium, Göttingen, Germany, September 11-17, 1992, pp. 285-288.
[26] Koumoutsakos, P., and Shiels, D., 1996, "Simulations of the Viscous Flow Normal to an Impulsively Started and Uniformly Accelerated Flat Plate," Journal of Fluid Mechanics, 328, pp. 177-227.
[27] Tonui, N., and Sumner, D., 2009, "Temporal Development of the Wake of a Non-Impulsively Started Circular Cylinder," Proceedings of the ASME 2009 Fluids Engineering Division Summer Meeting, August 2-5, 2009, Vail, Colorado, USA, Paper No. FEDSM2009-78018 (8 pages).

